Molecular Cancer Research

HIC1 Tumor Suppressor Loss Potentiates TLR2/NF-κB Signaling and Promotes Tissue Damage–Associated Tumorigenesis

Lucie Janeckova[1], Vendula Pospichalova[1], Bohumil Fafilek[1], Martina Vojtechova[1], Jolana Tureckova[1], Jan Dobes[1], Marion Dubuissez[2], Dominique Leprince[2], Nikol Baloghova[1], Monika Horazna[1], Adela Hlavata[1], Jitka Stancikova[1], Eva Sloncova[1], Katerina Galuskova[1], Hynek Strnad[1], and Vladimir Korinek[1]

Abstract

Hypermethylated in cancer 1 (*HIC1*) represents a prototypic tumor suppressor gene frequently inactivated by DNA methylation in many types of solid tumors. The gene encodes a sequence-specific transcriptional repressor controlling expression of several genes involved in cell cycle or stress control. In this study, a *Hic1* allele was conditionally deleted, using a Cre/loxP system, to identify genes influenced by the loss of Hic1. One of the transcripts upregulated upon Hic1 ablation is the *toll-like receptor 2* (*TLR2*). *Tlr2* expression levels increased in Hic1-deficient mouse embryonic fibroblasts (MEF) and cultured intestinal organoids or in human cells upon *HIC1* knockdown. In addition, HIC1 associated with the *TLR2* gene regulatory elements, as detected by chromatin immunoprecipitation, indicating that *Tlr2* indeed represents a direct Hic1 target. The Tlr2 receptor senses "danger" signals of microbial or endogenous origin to trigger multiple signaling pathways, including NF-κB signaling. Interestingly, Hic1 deficiency promoted NF-κB pathway activity not only in cells stimulated with Tlr2 ligand, but also in cells treated with NF-κB activators that stimulate different surface receptors. In the intestine, Hic1 is mainly expressed in differentiated epithelial cells and its ablation leads to increased Tlr2 production. Finally, in a chemical-induced mouse model of carcinogenesis, Hic1 absence resulted in larger Tlr2-positive colonic tumors that showed increased proportion of proliferating cells.

Implications: The tumor-suppressive function of Hic1 in colon is related to its inhibitory action on proproliferative signaling mediated by the Tlr2 receptor present on tumor cells. *Mol Cancer Res; 13(7); 1139–48. ©2015 AACR.*

Introduction

The *HIC1* gene was isolated as a candidate tumor suppressor gene during tumor DNA hypermethylation screen of the chromosome 17 short arm, a chromosomal region which is frequently reduced to homozygosity in human cancers (1). $Hic1^{-/-}$ mice die prenatally due to severe developmental defects of craniofacial structures and limbs (2). $Hic1^{+/-}$ mice are viable; however, they develop spontaneous malignant tumors that are Hic1 deficient due to the intact *Hic1* allele methylation (3). Hic1 protein functions as an evolutionarily conserved transcription repressor, which cooperates with several partners to regulate expression of multiple target genes (4). The protein is composed of three structural domains. The Broad complex, Tramtrack, Bric à brac/POx viruses, and Zinc finger (BTB/POZ) domain responsible for Hic1 multimerization is situated N-terminally, followed by the central region binding co-repressors such as C-terminal binding protein (CtBP). The C-terminal domain consists of five zinc fingers providing affinity to the specific Hic1-responsive (HiRE) sequence motif in DNA (5). The known Hic1 target genes participate in diverse cellular processes, including cell-cycle regulation, cell differentiation, DNA damage response, and metastatic invasion (reviewed in ref. 4). *Hic1* transcription is positively regulated by p53 protein, a key molecule inducing either cell-cycle arrest or apoptosis upon various cellular stress-inducing insults (6). Conversely, the p53 activity is restrained by a protein deacetylase encoded by the *sirtuin 1* (*Sirt1*) gene, whose expression is blocked by Hic1. *Hic1* inactivation thus leads to functional suppression of p53, allowing damaged cells to escape the p53-mediated response (7). Besides the direct regulation of gene expression, Hic1 attenuates transcription via interaction with other transcription factors. For example, association with Wnt pathway effector T-cell factor 4 (TCF4) sequesters TCF4 (and its transcriptional activator β-catenin) to nuclear speckles called Hic1 bodies. Subsequently, expression of the TCF4/β-catenin-responsive genes is inhibited (8).

The tissue maintenance of the single-layer intestinal epithelium is sustained by intestinal stem cells (ISC) that reside at the bottom

[1]Institute of Molecular Genetics, Academy of Sciences of the Czech Republic, Prague, Czech Republic. [2]CNRS UMR 8161, Institut de Biologie de Lille, Université Lille Nord de France, Institut Pasteur de Lille, Lille Cedex, France.

Note: Supplementary data for this article are available at Molecular Cancer Research Online (http://mcr.aacrjournals.org/).

Current address for V. Pospichalova: Faculty of Science, Masaryk University, Kotlarska 2, 611 37 Brno, Czech Republic.

Corresponding Author: Vladimir Korinek, Institute of Molecular Genetics AS CR, Videnska 1083, 142 20 Prague 4, Czech Republic. Phone: 420-241063146; Fax: 420-244472282; E-mail: korinek@img.cas.cz

doi: 10.1158/1541-7786.MCR-15-0033

of invaginations called intestinal crypts, where ISCs divide regularly and give rise to transit amplifying cells (TA). Rapidly dividing TA cells migrate upward and while exiting the crypt, they differentiate to absorptive enterocytes, mucus-producing goblet cells, and hormone-secreting enteroendocrine cells. In the small intestine, differentiated cells cover finger-like protrusions called villi; the surface of the colon is flat. The intestinal epithelium self-renewing in 3 to 5 days represents one of the most rapidly self-renewing tissues in the mammalian body. One exception from the outlined scheme are Paneth cells that secrete bactericidal cryptidins, defensins, or lysozyme. These relatively long-lived cells are present in the small intestine only. Moreover, during maturation, the Paneth cell does not migrate from the crypt but stays at the crypt bottom, where it persists for 6 to 8 weeks (reviewed in ref. 9). Owing to the dynamic turnover, the intestinal epithelium is at high risk of carcinogenesis. Although aberrant activation of the Wnt pathway initiates the majority of colorectal carcinomas (reviewed in ref. 10), CRC development is a multistep process that entails accumulation not only of genetic, but also of epigenetic changes in epithelial cells (11). The physiologic role of HIC1 in the intestine has not yet been elucidated in detail. However, in the mouse, Hic1 represses *atonal homolog 1* (*Atoh1*) and *SRY-box containing gene 9* (*Sox9*) genes, which are involved in the cell fate determination of secretory cell lineages in the small intestine (12–14).

In the present study, we used a conditional knock-out of the *Hic1* gene (15) to identify genes repressed by Hic1. Expression profiling of mouse embryonic fibroblasts (MEF) revealed six novel Hic1 target genes, including *Tlr2*. Tlr2 functions as a microbial sensor to initiate inflammation and immune responses. In addition, the receptor recognizes endogenous inflammatory mediators released from dead cells (review in ref. 16). Upon ligand binding, Tlr2 triggers several signal transduction pathways, including NF-κB signaling that activates expression of proinflammatory cytokines and enzymes, such as tumor necrosis factor-alpha (TNFα), interleukin 6 (IL6), and cyclooxygenase-2 (Cox2) (17). Solid tumors contain inflammatory infiltrates, and many recent studies have shown association between inflammation and increased risk of cancer development and progression. Furthermore, there is growing evidence that Tlr2 activators released from cancer cells might initiate persistent inflammation found in many tumors (reviewed in ref. 18). However, two recent studies documented an inflammation-independent Tlr2 role in promoting gastric and intestinal cancer (17, 19). Here, we show that *Hic1* depletion in the intestinal epithelium resulted in increased Tlr2 expression that promoted proliferation of colonic tumors induced by chemical carcinogenesis.

Materials and Methods

Experimental mice

Housing of mice and *in vivo* experiments were performed in compliance with the European Communities Council Directive of 24 November 1986 (86/609/EEC) and national and institutional guidelines. Animal care and experimental procedures were approved by the Animal Care Committee of the Institute of Molecular Genetics (Ref. 82/2011). Generation and genotyping of $Hic1^{flox/flox}$ and Hic1 citrine reporter ($Hic1^{cit/+}$) mice was described previously (15). The *Rosa26-CreERT2* [B6.129-Gt (ROSA)26Sor$^{tm1(cre/ERT2)Tyj}$/J] mouse strain was purchased from The Jackson Laboratory and was genotyped as recommended by the provider. *Villin-CreERT2* and *Villin-Cre* transgenic mice (20) were kindly provided by Sylvie Robine (Institut Curie, Centre de Recherche, Paris, France). Animals were housed in specific pathogen-free conditions. Tumors of the colon and rectum were collected from adult $Hic1^{flox/flox}$ *Villin-Cre*$^{+}$ mice 5 weeks after a single subcutaneous injection of azoxymethane [(AOM); 10 mg/kg; purchased from Sigma] that was followed by a 5-day dextran sodium sulfate (DSS) treatment in drinking water [2% (w/v) DSS; MW 36–50 kDa; MP Biomedicals]. The mice were euthanized and the intestines were dissected, washed in PBS, and fixed in 4% formaldehyde (v/v) in PBS for 3 days. Fixed intestines were embedded in paraffin, sectioned and stained. The number and size of the neoplastic lesions were quantified using Ellipse software (ViDiTo). Colitis was induced by DSS (2% in the drinking water for 5 days) without AOM treatment. Colons were collected 2, 6, and 9 days upon DSS withdrawal.

Cell and organoid culture, 4-hydroxytamoxifen (4-OHT) treatment

MEFs were isolated from embryos obtained at embryonic day (E) 11 to E14, details of the procedure are given in Supplement. For Cre-mediated recombination, cells were cultured in the presence of 4-OHT at a final concentration of 2 μmol/L (prepared from 1 mmol/L solution in ethanol; Sigma). Control cells were treated with the corresponding amount of ethanol. Small intestinal crypts were isolated and cultured according to the previously published protocol (21). Colonic crypts were isolated using the same procedure, but the culture medium was additionally supplemented with conditioned medium obtained from mouse Wnt3a-producing L cells (L-Wnt3a; ref. 22). L-Wnt3a, HEK293, and BJ-Tert cells were purchased from the ATCC (Cat. No.: CRL-2647, CRL-1573, and CRL-4001, respectively). All cell lines were obtained in 2006 and maintained in DMEM (Sigma) supplemented with 10% FBS (Gibco), penicillin, streptomycin, and gentamicin (Invitrogen). Upon receipt, cells were expanded and aliquots of cells at passage number <10 were stored frozen in liquid nitrogen. Cells from one aliquot were kept in culture for less than 2 months after resuscitation. The cell identity was not authenticated by the authors.

Microarray analysis

Total RNA was isolated from MEFs harvested 24, 48, 72, and 120 hours upon 4-OHT addition using RNeasy Plus Mini Kit (Qiagen). Control cells were grown with the same volume of vehicle (ethanol). The quality of isolated mRNA was checked using Agilent Bioanalyzer 2100; RNAs with RNA integrity number (RIN) above 8 were further processed. Two biologic replicates were used for each time point and treatment. The RNA samples were analyzed using MouseRef-8 v2.0 Expression BeadChip (Illumina). Raw data were processed using the beadarray package of Bioconductor and analyzed as described previously (23). Gene set enrichment analysis (GSEA) was performed using the Enricher gene analysis tool (http://amp.pharm.mssm.edu/Enrichr; ref. 24). Microarray data were deposited in ArrayExpress (http://www.ebi.ac.uk/arrayexpress) under accession number E-MTAB-3486.

Luciferase reporter assay, biochemistry, RNAi

MEFs were electroporated (details are given in Supplement); transfection of HEK293 cells was performed using Lipofectamine 2000 reagent (Invitrogen). Luciferase reporter constructs NF-κB-Luc and pRL-TK were purchased from Promega. To generate Tlr2-Luc reporter plasmid, genomic DNA containing the mouse Tlr2 promoter region encompassing nucleotides −796 to +52 (the

transcription start site corresponds to position +1) was amplified by PCR and cloned into the pGL4.26 luciferase reporter vector (Promega). The HIC1 construct was described previously (8). Details of the luciferase assay and NF-κB pathway stimulation are given in Supplement. For RNAi, BJ-Tert fibroblasts were reverse-transfected with Lipofectamine RNAiMax (Invitrogen) according to manufacturer's instructions using 10 nmol/L small interfering RNA (siRNA) targeting *HIC1* (HIC1 siGENOME SMART Pool M-006532-01, Dharmacon) or a scrambled control siRNA (siCtrl; siGENOME RISC free control siRNA, Dharmacon) and harvested 2 days upon transfection.

ChIP and droplet digital PCR

Chromatin immunoprecipitation (ChIP) using chromatin obtained from immortalized BJ-Tert fibroblasts was performed as described previously (25). Occupancy of gene regulatory regions by HIC1 was assayed by ddPCR (QX200, Bio-Rad) using EvaGreen master mix (Bio-Rad). PCR primers are listed in Supplement.

FACS

Paneth cell sorting was performed according to the previously published protocol (26). Antibodies used for flow cytometry: phycoerythrin (PE)-conjugated anti-CD24 (12-0242-81, eBioscience), allophycocyanin (APC)-conjugated anti-EpCam (17-5791-80, eBioscience), FITC-conjugated anti-CD45 (ED7018, ExBio).

IHC

The technique was performed as described previously (27, 28). Hematoxylin and eosin (Sigma) were used for counterstaining. Antibodies are given in Supplement. For visualization of citrine fluorescence, intestines dissected from $Hic1^{cit/+}$ and wild-type (wt) mice were snap frozen in liquid nitrogen and immediately sectioned. Specimens were stained with 4′,6-diamidino-2-phenylindole, dihydrochloride (DAPI; Life Technologies) and the citrine fluorescence signal was evaluated using a laser scanning confocal microscope (Leica TCS SP5).

Western blotting and antibodies

Hic1-specific polyclonal antisera were generated in rabbit or chicken immunized with the recombinant His-tagged fragment of human HIC1 protein (amino acids 154-396). Commercially available antibodies are given in Supplement.

RNA purification and reverse-transcription quantitative PCR

Total RNAs were isolated from cells and tissues using RNeasy Mini Kit (Qiagen) and reversely transcribed and analyzed by qRT-PCR as described previously (29). The primers are listed in Supplementary Table S1.

Statistical analysis of data

Results of the gene reporter assay, Ellipse, and qRT-PCR analysis were evaluated by the Student *t* test. Datasets obtained using DNA microarrays were analyzed in the R environment using the package LIMMA (Linear Models for Microarray Data LIMMA; ref. 30).

Results

Identification of *Tlr2* as a novel target gene repressed by Hic1 in mouse and human cells

To investigate the biologic function of transcription repressor Hic1, we have recently developed the $Hic1^{flox/flox}$ mouse strain that enables conditional inactivation of the *Hic1* gene (15). These mice were crossed to *Rosa26-CreERT2* animals expressing Cre recombinase estrogen receptor T2 fusion protein (CreERT2) from the *Rosa26* locus (31). The fusion protein resides in the cytoplasm until an antagonist of the estrogen receptor, tamoxifen (or its active metabolite 4-OHT), is administered. Subsequently, Cre enzyme is translocated into the nucleus, where it allows excision of DNA sequences flanked, that is, "floxed", by loxP sites (32). MEFs were isolated from embryos, cultured with 4-OHT or vehicle (ethanol) and genotyped by PCR to confirm locus recombination and generation of the $Hic1^{delEx2}$ allele. Simultaneously, the presence of Hic1 protein was detected by immunoblotting (Fig. 1A). Subsequently, total RNA was isolated at four time points after the addition of 4-OHT (or vehicle) into the culture media, and microarray analysis of the expression profile was performed. The analysis revealed genes whose expression was changed significantly ($q < 0.05$) after the *Hic1* locus recombination. Furthermore, six genes were upregulated in at least two time points and more than twice [the binary logarithm of fold change (log FC) > 1; Fig. 1B and Supplementary Fig. S1 and Supplementary Table S2]. These genes were *angiopoietin-like 7* (*Angptl7*), *carbonyl reductase 2* (*Cbr2*), *death-associated protein kinase 2* (*Dapk2*), *HSP, α-crystallin-related, B6* (*Hspb6*), *Tlr2*, and *WAP four-disulfide core domain 2* (*Wfdc2*). In addition, increased expression of previously identified HIC1 target genes *cyclin-dependent kinase inhibitor 1a* (*CDKN1A*; ref. 33), *Sox9* (13), and *Sirt1* (7) was observed, but these genes did not satisfy the significance criteria (not shown). Rather unexpectedly, the GSEA analysis using the Enricher gene library online tool (24) revealed that the inactivation of the *Hic1* gene in MEFs mainly altered expression of genes involved in lipid metabolism (Supplementary Table S3).

As recent evidence supports the role of TLR signaling in inflammation-associated tumorigenesis in the gastrointestinal tract (reviewed in ref. 34), we further investigated the relationship between Hic1 and *Tlr2* expression. First, we generated a Tlr2-Luc reporter by subcloning genomic DNA harboring the *Tlr2* promoter region before the luciferase sequence. Then, we cotransfected the Tlr2-Luc reporter together with the expression construct encoding HIC1 into HEK293 cells and performed the luciferase reporter assay. As expected, increasing amounts of HIC1 resulted in reduced activity of the reporter, whereas cotransfection with a control "empty" plasmid had no significant effect (Fig. 1C). Moreover, we used a HIC1-specific antibody to perform ChIP using chromatin isolated from BJ fibroblasts that express detectable amounts of endogenous HIC1 (25). Droplet digital PCR confirmed the enrichment of genomic DNA encompassing the promoter regions of *TLR2* and *SIRT1* (used as positive control) genes in the precipitate. Importantly, none of these regions was precipitated using a control "irrelevant" antibody and, furthermore, the anti-HIC1 antibody did not pull down the *β-ACTIN* promoter used as negative control. In addition, upregulation of *TLR2* and *SIRT1* was detected upon *HIC1* mRNA knockdown (Fig. 1D and data not shown). The *Tlr2* gene is activated by NF-κB signaling (35); therefore, the luciferase assay was performed in MEFs stimulated with NF-κB pathway activators TNFα, LTα, and with synthetic bacterial lipopeptide Pam3csk4, which functions as the Tlr2 ligand (36). Interestingly, Pam3csk4 appeared to be the most potent enhancer of the Tlr2-Luc activity, especially upon Hic1 deletion; however, the Tlr2-Luc activity was also significantly increased upon stimulation with unrelated LTα. In addition, the luciferase reporter assay clearly showed increased Tlr2-Luc activity

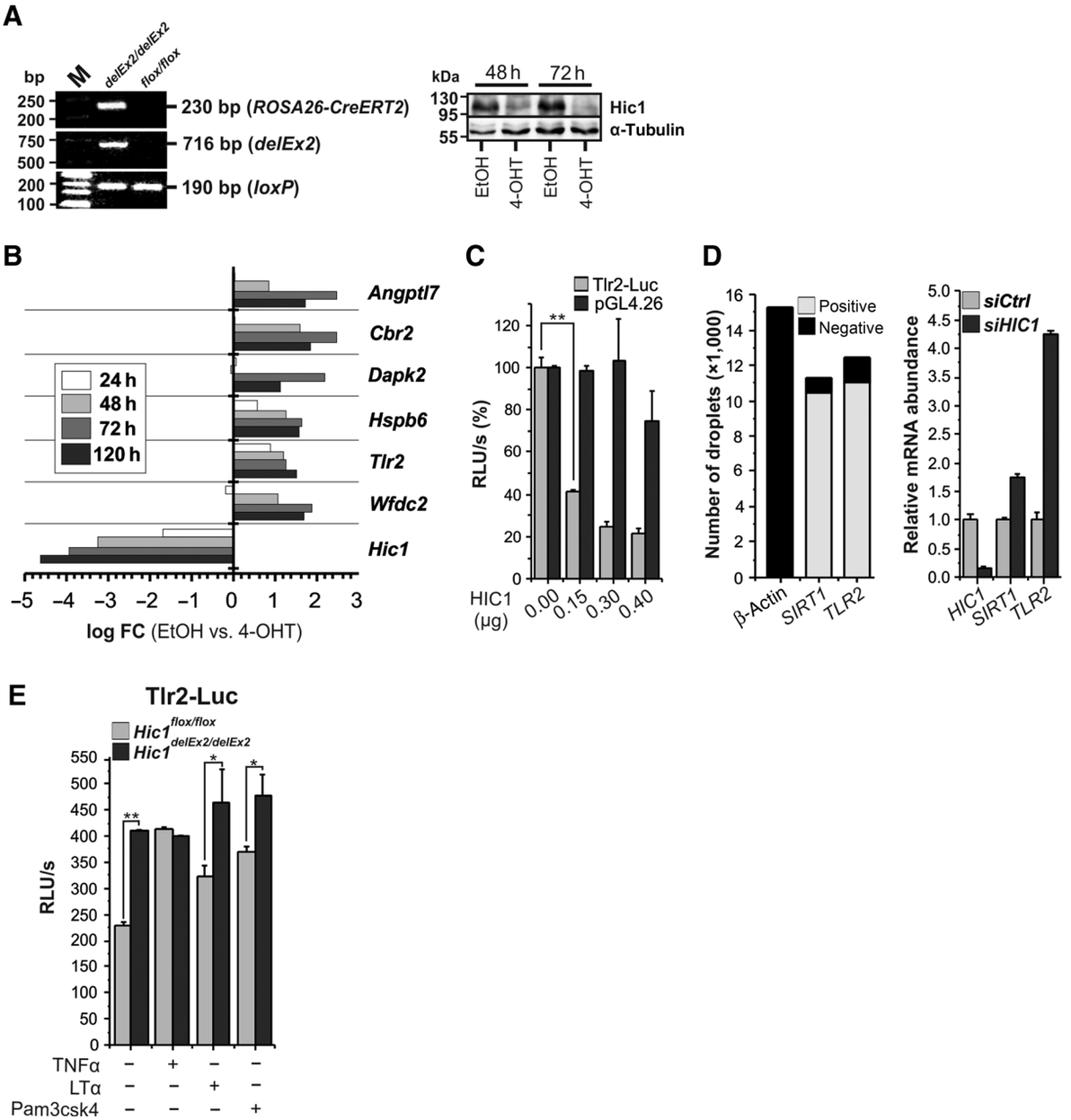

Figure 1.

Tlr2 represents a novel direct target gene of transcriptional repressor Hic1. A, left, PCR genotyping of MEFs isolated from *Hic1*$^{flox/flox}$ *Rosa26*$^{CreERT2/+}$ embryos. Cells were cultured with 4-OHT for 4 days. PCR on the homozygous *flox/flox* and hemizygous *CreERT2* allele produced 190 bp or 230 bp DNA fragments, respectively. Cre-mediated recombination generated the *delEx2* allele lacking the second *Hic1* exon encoding the major part of the protein. The recombination is documented by the presence of the 716-bp PCR product. Right, immunoblotting of *Hic1*$^{flox/flox}$ *Rosa26*$^{CreERT2/+}$ cell lysates obtained from MEFs 48 and 72 hours after adding 4-OHT or solvent [ethanol (EtOH)]. Western blotting with an anti–α-tubulin antibody was used as a loading control. B, expression profile of *Hic1*$^{delEx2/delEx2}$ MEFs compared to *Hic1*$^{flox/flox}$ cells at the indicated time points after adding 4-OHT. The decrease in *Hic1* mRNA levels was accompanied by significant upregulation ($q < 0.05$) of six genes; log FC, binary logarithm of fluorescent intensity of the indicated gene-specific probe upon hybridization with labeled RNA isolated from MEFs treated with 4-OHT versus fluorescent intensity obtained using RNA isolated from cells treated with vehicle only. C, luciferase reporter assays in HEK293 cells cotransfected with the Tlr2-Luc reporter or control vector pGL4, respectively, together with increasing amounts of HIC1-producing plasmid. D, left, ddPCR using genomic DNA obtained from human BJ cells by ChIP with an anti-HIC1 antibody. Although PCR using primers designed from the promoter regions of *SIRT1* and *TLR2* genes, that is, genes directly repressed by HIC1, produced mainly droplets containing a PCR product, PCR with primers designed from the *β-ACTIN* promoter gave droplets without any product. Right, qRT-PCR analysis of BJ cells upon HIC1 knockdown. Expression level of the respective gene in cells treated with non-silencing siRNA (siCtrl) was set to 1. E, luciferase reporter assays in MEFs electroporated with Tlr2-Luc reporter plasmid. Cells were stimulated overnight with TNFα, LTα, or Pam3csk4. The histograms represent average luciferase light units per second (RLU/s) obtained in three independent experiments performed in triplicates. The values were corrected for efficiency of electroporation using *Renilla* luciferase as the internal control. Error bars represent SDs; *, $P < 0.05$; **, $P < 0.01$.

in Hic1-deficient MEFs when compared with cells with the intact *Hic1* locus (Fig. 1E). Several studies indicate the NF-κB pathway activation via Tlr2 signaling (37, 38). Thus, we next examined the consequence of *Hic1* deficiency for the NF-κB pathway. Luciferase reporter assay using the NF-κB-Luc reporter showed increased NF-κB signaling even in unstimulated $Hic1^{delEx2/delEx2}$ cells (compared with MEFs before Cre-mediated *Hic1* inactivation). Treatment of cells with Pam3csk4 further potentiated the reporter activity. However, increased NF-κB signaling was also observed upon stimulation with LTα and TNFα, indicating that the NF-κB pathway output was not completely dependent on Tlr2 (over) expression (Fig. 2A). The augmentation of the NF-κB pathway activity in Hic1-deficient MEFs was confirmed by qRT-PCR analysis that showed increased expression of the putative NF-κB target genes *Cox2* and *TNFα* (Fig. 2B). In agreement with these results, immunoblotting revealed increased levels of the phosphorylated transcriptionally active form of the nuclear mediator of NF-κB signaling p65 (Fig. 2C). In summary, all the data supported direct transcriptional repression of *Tlr2* by Hic1 and, moreover, potentiation of the NF-κB pathway activity upon loss of the *Hic1* gene.

Hic1 depletion in the intestinal epithelium results in *Tlr2* upregulation

In the intestinal epithelium, the *Hic1* expression was examined using previously generated Hic1-citrine "reporter" mice. In this mouse strain, the sequence encoding the central and C-terminal portions of Hic1 protein was replaced by cDNA encoding citrine (yellow) fluorescent protein (15). In both the small and large intestine, native citrine fluorescence was observed in epithelial cells (Fig. 3A). Subsequently, production of Hic1 protein in the gut epithelia was confirmed by immunoblotting using cell lysates prepared from crypts and differentiated cells lining the villi in the small intestine or intercrypt regions (ICR) in the colon. The analysis revealed higher amounts of Hic1 in the villus and ICR fractions when compared with the crypts. This result was confirmed by qRT-PCR using total RNA isolated from the same epithelial fractions (Fig. 3B). In order to evaluate the expressional changes of the putative Hic1 target genes in epithelial cells, we established three-dimensional "organoid" cultures (21) from the small intestinal crypts of $Hic1^{flox/flox}$ *Villin-CreERT2*$^{+}$ mice producing tamofixen-regulated Cre enzyme in all intestinal cell lineages (20). Interestingly, Cre-mediated inactivation of the *Hic1* gene increased mRNA levels of all genes identified by the microarray analysis. Furthermore, like in MEFs, Hic1 deficiency resulted in upregulation of the NF-κB-responsive genes *Cox2* and *TNFα* (Fig. 3C). In addition, Tlr2 was analyzed in $Hic1^{flox/flox}$ *Villin-Cre*$^{+}$ mice expressing the constitutively active form of Cre enzyme in the embryonic and adult gut epithelia (20). Although efficient recombination and generation of the $Hic1^{delEx2}$ allele along the rostrocaudal axis of the gastrointestinal tract was confirmed by PCR genotyping (data not shown), these mice—lacking *Hic1* in the intestinal epithelium—were viable, showing no signs of any health problems. However, IHC staining showed increased Tlr2 positivity in the small intestine and colon (Fig. 3D).

Hic1-deficient intestinal epithelium contains increased numbers of secretory cell lineages

As morphology and proliferation of the $Hic1^{loxP/loxP}$*Villin-Cre*$^{+}$ intestinal epithelium appeared to be normal, we performed detailed analysis of all major cellular lineages present in the small intestine. Maturation of Paneth cells is driven by transcription factors *Atoh1* and *Sox9* (14). Interestingly, Hic1 is a transcriptional repressor of *Atoh1* and *SOX9* in the mouse developing cerebellum and in U2OS osteosarcoma cells, respectively (12, 13). Using

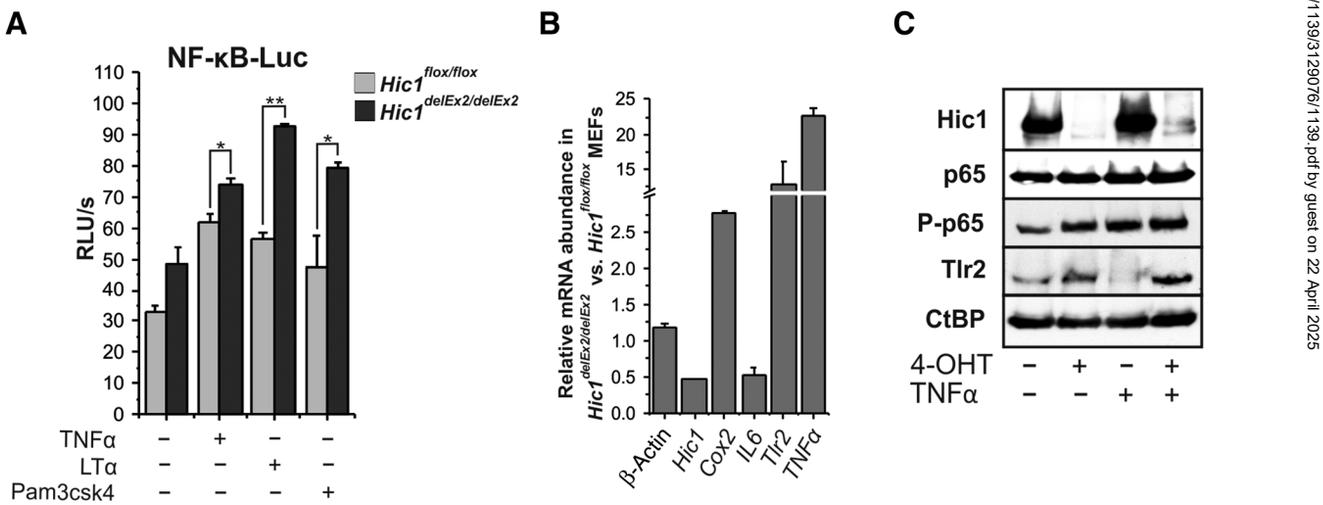

Figure 2.
Hic1-deficient MEFs display upregulated NF-κB signaling. A, luciferase reporter assays in MEFs cultured with 4-OHT or vehicle (ethanol) for 3 days and then electroporated with the NF-κB-Luc reporter. Six hours upon electroporation, TNFα, LTα, or Pam3csk4 was added to the culture medium and the cells were harvested 12 hours later. The assay was performed in triplicates, representative results are shown. *, $P<0.05$; **, $P < 0.01$. B, qRT-PCR analysis of putative target genes of NF-κB signaling *Cox2*, *IL6*, and *TNFα* in *Hic1*-deficient or control vehicle-treated MEFs. Total RNA was isolated from cells cultured with 4-OHT or vehicle for 3 days and then stimulated with the indicated ligand overnight. The results were normalized to the *Ubiquitin B* (*Ubb*) housekeeping gene; the relative expression of another housekeeping gene, *β-actin*, is also shown. The expression level of the respective gene in control vehicle-treated cells was arbitrarily set to 1. The analysis was performed in triplicates; error bars: SDs. C, immunoblotting of lysates prepared from MEFs cultured with 4-OHT or vehicle for 3 days and then stimulated with TNFα for 30 minutes. The experiment was repeated twice, representative blot is presented. CtBP, loading control; P-p65, immunoblotting with an antibody recognizing p65 phosphorylated at S536.

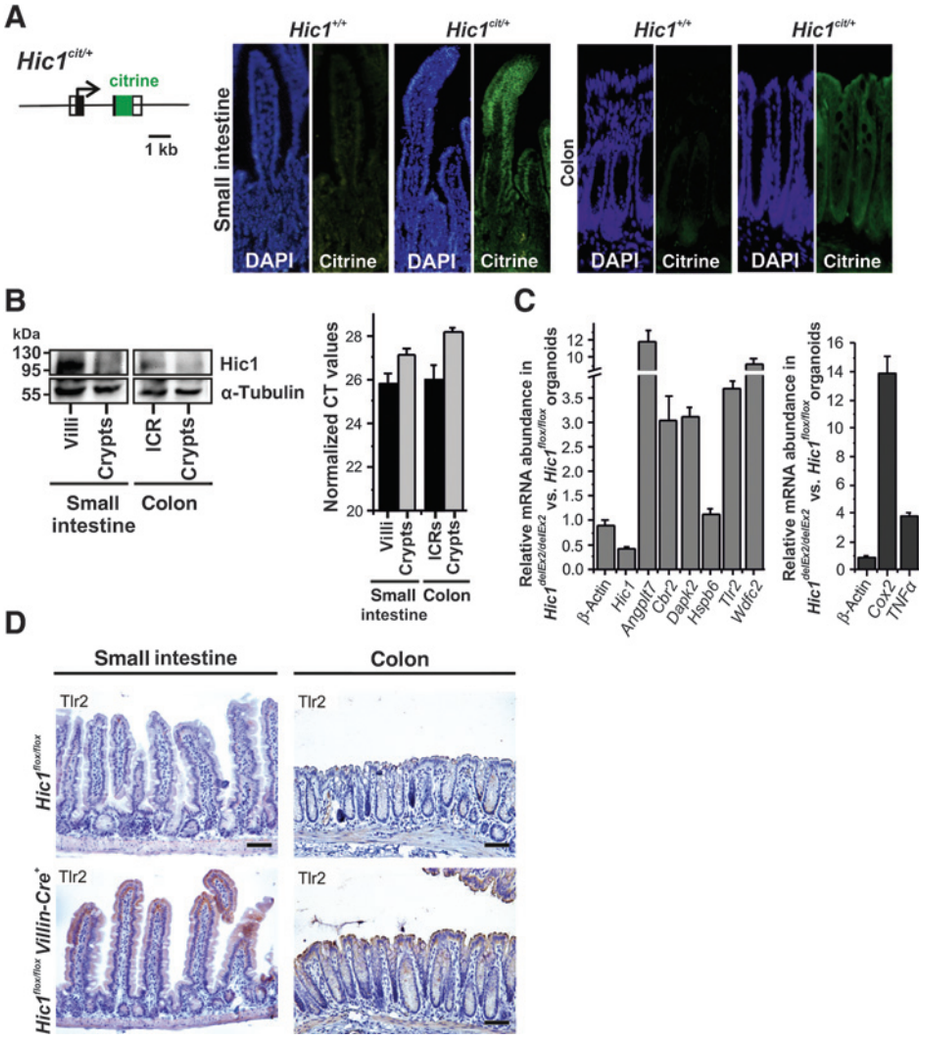

Figure 3.
Increased expression of *Tlr2* in *Hic1*-deficient small intestinal organoids and intestinal epithelia. A, production of Hic1-citrine fusion protein in $Hic1^{cit/+}$ mouse is restricted to the epithelium of the small intestine and colon. Left, a scheme of the *Hic1-citrine* reporter allele producing citrine fluorescent protein from the *Hic1* locus. Exons are depicted by boxes; coding sequences are filled, arrow indicates the transcription start site. Right, fluorescent microphotographs of cryosections of the small intestine and colon of $Hic1^{+/+}$ and $Hic1^{cit/+}$ mouse counterstained with DAPI nuclear stain (blue fluorescence). The right image from each pair was gained in "citrine" (green fluorescence) channel to monitor expression from the *Hic1* locus. No citrine fluorescence was observed in the intestine of control $Hic1^{+/+}$ animals. B, left, Western blotting from separated epithelial lining of the wt small intestinal villi and crypts and from the wt intercrypt regions (ICRs) and crypts of the colon; α-tubulin, loading control. Right, qRT-PCR analysis of total RNA isolated from the indicated regions of the intestinal epithelium. Cycle threshold (C_t) values normalized to *Ubb* are shown. C, qRT-PCR analysis of RNA isolated from organoids established from the small intestinal crypts of $Hic1^{flox/flox}$ *Villin-CreERT2*$^{+}$ mice. Vehicle (EtOH) or 4-OHT was added to the culture medium third day after the crypt isolation and the organoids were harvested after another 3 days. The expression level of the respective gene in vehicle-treated organoids was arbitrarily set to 1. The scheme represents results obtained in two independent experiments (each) performed in triplicates. Errors bars: SDs. D, IHC staining of Tlr2 [brown 3,3′-Diaminobenzidine (DAB) stain] in $Hic1^{flox/flox}$ and $Hic1^{flox/flox}$ *Villin-Cre*+ intestines. The specimens were counterstained with hematoxylin (blue nuclear stain). Scale bar: 0.15 mm.

expression profiling of sorted Paneth cells isolated from the $Hic1^{flox/flox}$ *Villin-Cre*$^{+}$ and control ($Hic1^{flox/flox}$) small intestinal crypts, we observed a significant increase in *Atoh1*, *Sox9*, and *Tlr2* mRNA levels upon loss of Hic1. Moreover, FACS analysis showed a slight increase in Paneth cell counts in $Hic1^{flox/flox}$ *Villin-Cre*$^{+}$ animals (Fig. 4A). Increased Paneth cell numbers along the rostrocaudal axis of the small intestine were also recorded using paraffin sections stained with an antibody recognizing Paneth cell-specific marker lysozyme (Fig. 4B). In addition, the numbers of mucin-producing goblet cells and chromogranin A-positive enteroendocrine cells were also elevated. In contrast, the differentiation and number of absorptive enterocytes seemed unchanged in the Hic1-deficient intestine (Supplementary Fig. S2).

Loss of Hic1 promotes colitis-associated tumorigenesis

Recently, Mohammad and colleagues described accelerated formation of tumors upon loss of *Hic1* in the $Apc^{Min/+}$ mouse model of intestinal cancer (39). Because inflammation is an important tumor promoter in colorectal neoplasia, the role of Hic1 was examined utilizing colitis-associated tumorigenesis. In

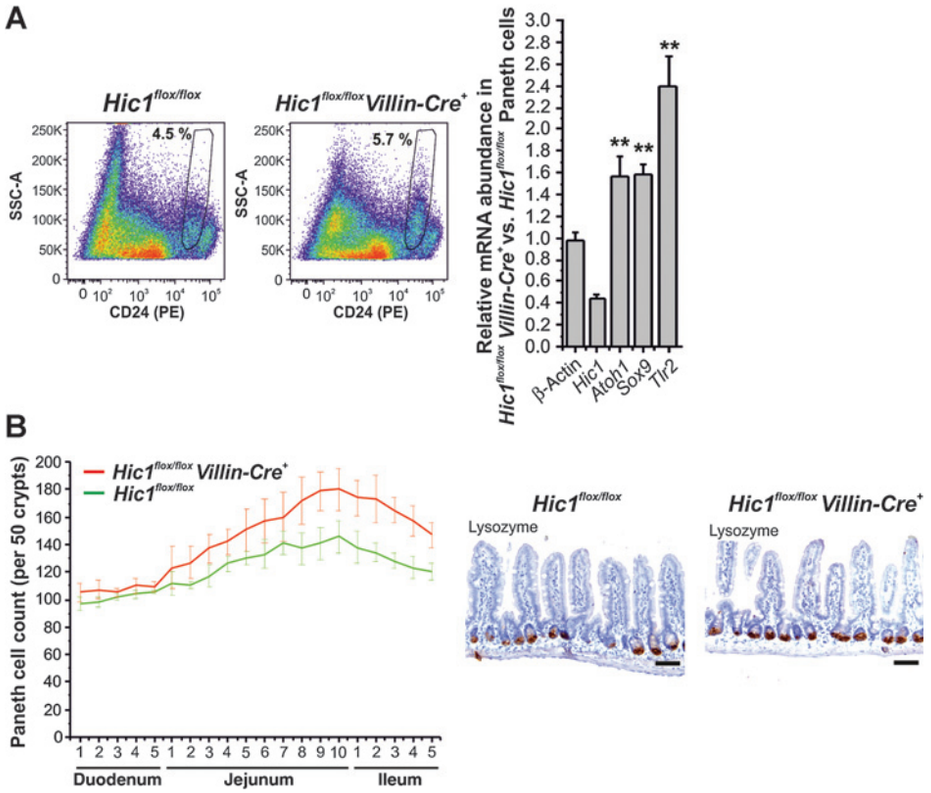

Figure 4.
Loss of the Hic1 function results in increased counts of Paneth cells. A, left, FACS analysis of Paneth cells obtained from the indicated mouse strains. Representative histograms show higher numbers of Paneth cells in the Hic1-deficient small intestine. Four animals per strain were used for the experiment. Right, qRT-PCR of sorted Paneth cells. Decreased *Hic1* expression results in upregulation of Hic1 target genes *Atoh1*, *Sox9*, and *Tlr2*. The expression level of the respective gene in *Hic1* wt cells was arbitrarily set to 1. **, $P < 0.01$. B, Paneth cell distribution in the indicated segments of the small intestine. Specimens obtained from four $Hic1^{flox/flox}$ and four $Hic1^{flox/flox}$*Villin-Cre*$^{+}$ mice were stained using an anti-lysozyme antibody to visualize Paneth cells (right images). Lysozyme-positive cells were counted in 50 neighboring crypts in several different fields indicated by numbers on the *x*-axis. Scale bar: 0.15 mm; error bars: SDs.

the acute colitis phase – induced by DSS treatment – no differences in the extent of tissue damage were observed in histologic specimens obtained from $Hic1^{flox/flox}$ *Villin-Cre*$^{+}$ and $Hic1^{flox/flox}$ mice. However, $Hic1^{flox/flox}$ *Villin-Cre*$^{+}$ individuals displayed more robust DSS treatment-associated transcriptional response of the *Cox2*, *Tlr2*, and *TNFα* genes, that is, genes upregulated upon *Hic*1 loss. Analysis of the colon during the regenerative phase, that is, 6 and 9 days upon DSS withdrawal, showed a more robust hyperproliferative response of the colonic epithelium of $Hic1^{flox/flox}$ *Villin-Cre*$^{+}$ individuals when compared with their $Hic1^{flox/flox}$ littermates (Fig. 5A). Moreover, a continuous increase of *Cox2*, *Tlr2*, and *TNFα* expression was observed at these time points (Supplementary Fig. S3). Strikingly, upon combined AOM/DSS treatment, Hic1 deficiency significantly increased the size of colonic and rectal tumors (Fig. 5B; average tumor size in $Hic1^{flox/flox}$ mouse = 3.1 mm^2 vs. 8.7 mm^2 in $Hic1^{flox/flox}$ *Villin-Cre*$^{+}$; $P = 0.00862$). IHC examination revealed decreased numbers of p53-positive cells within the tumor mass of *Hic1*-negative mice. Nevertheless, even in $Hic1^{flox/flox}$ mice, cells displaying nuclear p53 staining were rare and scattered throughout the neoplastic tissue. However, expression of the p21 cell-cycle inhibitor, the most prominent in wt cells at the surface area of the tumors, was reduced in *Hic1* knock-outs. Strikingly, proliferating cell nuclear antigen (PCNA) expressing cells were localized in wt mice in areas clearly distinguished from the regions containing p21-positive cells. In contrast, in Hic1-deficient mice, proliferating cells were more abundant and dispersed throughout the neoplastic tissue. Finally, no differences were noted in the numbers of apoptotic cells (Fig. 5C and not shown).

Discussion

In the present study, we used a gene inactivation-based screen to identify genes regulated by the Hic1 tumor suppressor. Interestingly, none of the identified presumptive Hic1 target genes was described previously. As the expression of all tested genes reacted to the Hic1 presence not only in MEFs, but also in intestinal organoids, we can exclude the possibility that the genes represent a small (sub)set of tissue-specific Hic1 targets. More likely, because the majority of previous studies utilized cells (over)producing ectopic HIC1 or cells treated with HIC1-specific siRNA (33), we suggest that (our) genes represent Hic1 target genes whose expression is relieved when the Hic1 steady-state levels are diminishing. On the other hand, the previously identified targets might represent genes efficiently repressed (or activated) immediately upon perturbation of the Hic1 protein levels. We used Hic1-reporter mice, Western blotting, and FACS analysis to demonstrate that in the adult intestine, Hic1 is mainly expressed in the differentiated epithelial cells. The expression of its target gene, *Tlr2*, was documented in ISCs (19). However, in the Hic1-deficient gut, Tlr2 was upregulated in differentiated cells, confirming the inverse Hic1-Tlr2 relationship. Moreover, intestinal ablation of *Hic1* resulted in a moderate increase in Paneth, goblet, and enteroendocrine cell numbers. Such phenotype might be attributed to upregulation of *Atoh1*, the Hic1 target gene functioning as the master regulator of secretory cell lineages in the small intestine (14). Upon ligand binding, Tlr2 triggers several signal transduction pathways, including NF-κB signaling (17). Interestingly, qRT-PCR analysis and luciferase reporter assays revealed that not only

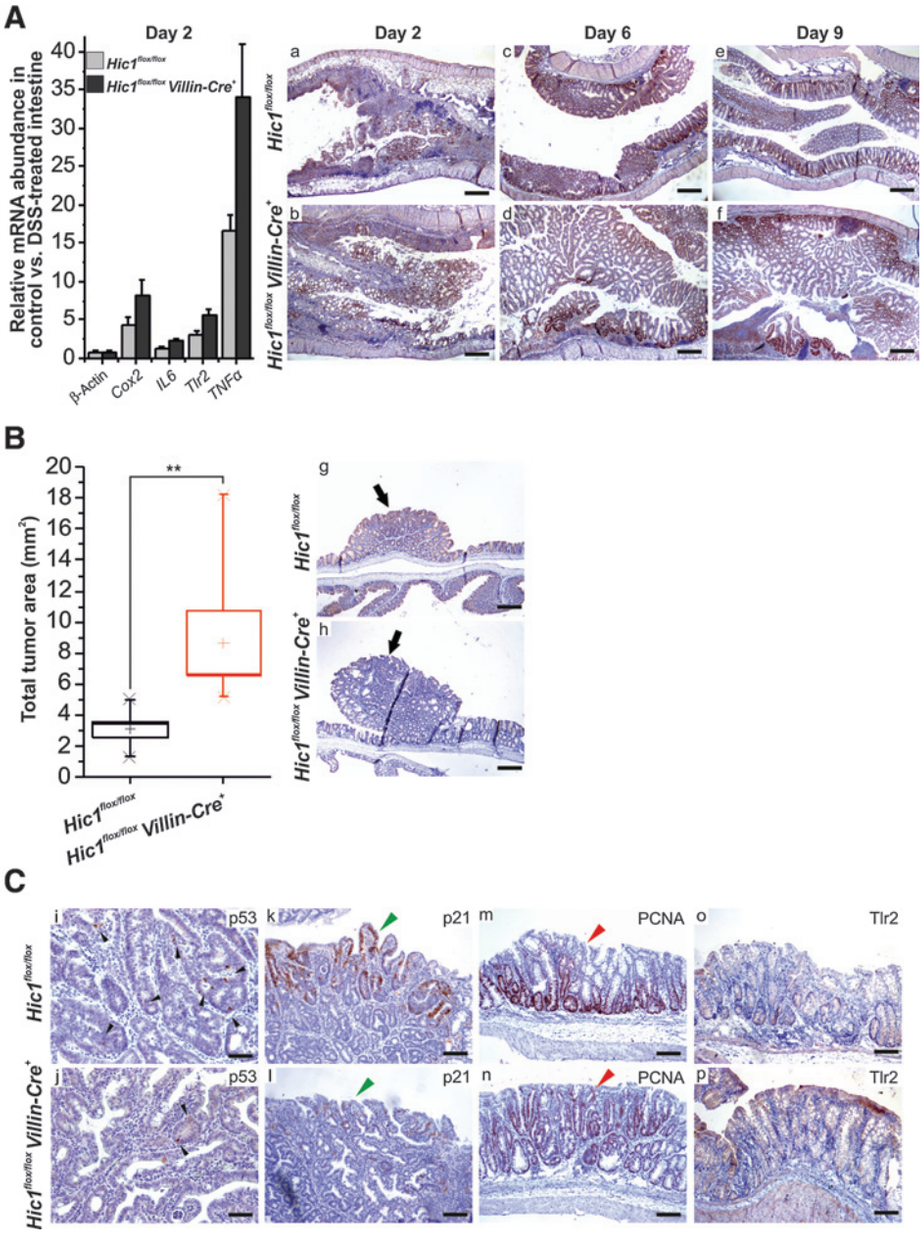

Figure 5.

Hic1 deficiency increased the size of colonic tumors generated upon AOM/DSS treatment. A, acute colitis and regeneration after DSS treatment. Left, DSS-induced transcriptional response in the colon of $Hic1^{flox/flox}$ and $Hic1^{flox/flox}$ *Villin-Cre*$^{+}$ mice 2 days upon DSS withdrawal. The expression level of the corresponding genes in mice without DSS treatment was arbitrarily set to 1. Four animals for each genotype were analyzed. Right, representative microscopic images of the colon two (a, b), six (c, d) and nine (e, f) days upon DSS withdrawal. The specimens were stained using an anti-PCNA antibody to detect proliferative cells (brown nuclear precipitate) and counterstained with hematoxylin (blue nuclear staining). B, tumor size in the colon generated in the indicated mouse strains upon combined AOM/DSS treatment. Intestines dissected from seven animals in each group were analyzed 5 weeks after the AOM/DSS application. Left, quantification of the total tumor area indicating significantly increased tumor burden in the *Hic1*-deficient colon. The total tumor area determined in each individual is indicated in the boxplots. The boxed areas correspond to the second and third quartiles; the spread of the values is given by "whiskers" above and below each box. Median (transverse line) and mean (cross) is marked inside each box. **, $P < 0.01$; error bars: SDs. Right, representative microscopic images of the colon; neoplastic outgrows are indicated by black arrows. The specimens were counterstained with hematoxylin and an anti–β-catenin antibody. C, IHC detection of tumor suppressor p53 [black arrowheads in panel (i) and (j)], cell-cycle inhibitor p21 [green arrowheads in (k) and (l)], PCNA-positive [(m, n); red arrowheads indicate differentially stained tumor surface] and Tlr2-producing (o, p) cells in colonic tumors. Scale bar: 0.75 mm (a–h); 0.15 mm (i, j); 0.3 mm (k-p).

ligand-induced, but also basal levels of the NF-κB signaling are elevated in Hic1-deficient cells (Fig. 2A and B). As the NF-κB pathway activity was more pronounced even in cells stimulated with other NF-κB inducers, the observed NF-κB (hyper)activity cannot be solely attributed to the increase in Tlr2 expression or function. Indeed, Western blotting confirmed that $Hic1^{delEx2/delEx2}$ cells displayed higher amounts of phosphorylated nuclear NF-κB mediator p65 (Fig. 2C). The exact reason(s) why Hic1 deficiency potentiates NF-κB signaling remains to be determined. Nevertheless, since several studies reported interaction between the STAT3 and NF-κB pathways (reviewed in ref. 40), we suggest that the autocrine IL6-STAT3 signaling might also be linked to the observed "boosts" in cellular reactivity to the stimuli activating the NF-κB pathway and to the increase in p65 stability and phosphorylation.

Several studies have demonstrated that *Tlr2* expression is increased during intestinal inflammation (41) or in human patients with ulcerative colitis (42). In addition, Maeda and colleagues showed that conditioned medium obtained from cultured colon cancer cells might activate NF-κB signaling via Tlr2 (43). These data are in accordance with our observation that in damaged tissue, transcription of *Tlr2* and genes linked to active NF-κB signaling is elevated. Importantly, in the *Hic1*-deficient colon, the damage-induced transcriptional response was more robust than in wt mice, supporting the Hic1 repressive role in *Tlr2* expression and NF-κB activation (Fig. 5A and Supplementary Fig. S3). Interestingly, several recent studies reported decreased tumor burden in $Apc^{+/Min}$ mice deficient in Tlr2 or its intracellular adaptor myeloid differentiation primary response protein-88 (Myd88; refs. 19, 44). Furthermore, deletion of *Tlr2* (or *Myd88*) reduced development of

colonic tumors in DSS-treated animals. Moreover, functional blocking of TLR2 inhibited *in vitro* growth of cancer cells (19). In another study, epithelial expression of Tlr2 and Tlr2/NF-κB signaling promoted growth and survival of gastric cancer cells (17). In summary, all these results support the cell-autonomous and inflammation-independent role of Tlr2 in cancer.

HIC1 participates in the cellular network regulating the DNA damage response (7). HIC1-mediated repression of deacetylase *SIRT1* gene promotes p53 stability and potentiates transcription of p53-dependent genes such as *p21* (45) and, in a positive regulatory feedback loop, also *HIC1* itself (1, 46). Unexpectedly, only a small fraction of cells in tumors generated by AOM/DSS treatment displayed stabilized p53 (Fig. 5C). Although the portion of p53-positive cells was decreased in *Hic1*$^{-/-}$ neoplastic tissues, it is unlikely that the increased tumor size observed upon Hic1 deletion is linked to the attenuated p53-mediated response. In human cells, HIC1 directly represses transcription of the *CDKN1A* gene encoding p21 (33). Strikingly, in Hic1-deficient tumors, we observed the opposite effect of Hic1 absence, that is, reduced p21 staining (Fig. 5C). Nevertheless, the observed discrepancy of the results might be explained by the fact that next to p53 and HIC1, p21 levels might be controlled by many other stimuli and also by post-transcriptional mechanisms (reviewed in ref. 47). As we noted increased cell proliferation upon DSS-induced epithelial damage and in Hic1-negative AOM/DSS tumors, we suggest that besides compromising the p53-mediated tumor-suppressive mechanisms the loss of Hic1 might potentiates tumor-promoting proproliferative Tlr2/NF-κB signaling.

Disclosure of Potential Conflicts of Interest

No potential conflicts of interest were disclosed.

Authors' Contributions

Conception and design: L. Janeckova, V. Pospichalova, V. Korinek
Development of methodology: V. Pospichalova, M. Dubuissez, D. Leprince, A. Hlavata, V. Korinek
Acquisition of data (provided animals, acquired and managed patients, provided facilities, etc.): L. Janeckova, V. Pospichalova, M. Vojtechova, J. Tureckova, J. Dobes, M. Dubuissez, D. Leprince, N. Baloghova, M. Horazna, A. Hlavata, J. Stancikova, E. Sloncova
Analysis and interpretation of data (e.g., statistical analysis, biostatistics, computational analysis): L. Janeckova, V. Pospichalova, A. Hlavata, H. Strnad, V. Korinek
Writing, review, and/or revision of the manuscript: L. Janeckova, V. Pospichalova, D. Leprince, V. Korinek
Administrative, technical, or material support (i.e., reporting or organizing data, constructing databases): K. Galuskova
Study supervision: V. Korinek

Acknowledgments

The authors thank S. Robine for Villin-Cre and Villin-CreERT2 mice, and S. Takacova for critically reading the manuscript.

Grant Support

This work was supported by Grant Agency of the Czech Republic Grant No. P305/12/2347, institutional Grant No. RVO 68378050, and project BIOCEV – Biotechnology and Biomedicine Centre of the Academy of Sciences and Charles University (CZ.1.05/1.1.00/02.0109) from the European Regional Development Fund.

The costs of publication of this article were defrayed in part by the payment of page charges. This article must therefore be hereby marked *advertisement* in accordance with 18 U.S.C. Section 1734 solely to indicate this fact.

Received January 19, 2015; revised March 20, 2015; accepted April 1, 2015; published OnlineFirst May 1, 2015.

References

1. Wales MM, Biel MA, el Deiry W, Nelkin BD, Issa JP, Cavenee WK, et al. p53 activates expression of HIC-1, a new candidate tumour suppressor gene on 17p13.3. Nat Med 1995;1:570–7.
2. Carter MG, Johns MA, Zeng X, Zhou L, Zink MC, Mankowski JL, et al. Mice deficient in the candidate tumor suppressor gene Hic1 exhibit developmental defects of structures affected in the Miller-Dieker syndrome. Hum Mol Genet 2000;9:413–9.
3. Chen WY, Zeng X, Carter MG, Morrell CN, Chiu Yen RW, Esteller M, et al. Heterozygous disruption of Hic1 predisposes mice to a gender-dependent spectrum of malignant tumors. Nat Genet 2003;33:197–202.
4. Rood BR, Leprince D. Deciphering HIC1 control pathways to reveal new avenues in cancer therapeutics. Expert Opin Ther Targets 2013; 17:811–27.
5. Pinte S, Stankovic-Valentin N, Deltour S, Rood BR, Guerardel C, Leprince D. The tumor suppressor gene HIC1 (hypermethylated in cancer 1) is a sequence-specific transcriptional repressor: definition of its consensus binding sequence and analysis of its DNA binding and repressive properties. J Biol Chem 2004;279:38313–24.
6. Guerardel C, Deltour S, Pinte S, Monte D, Begue A, Godwin AK, et al. Identification in the human candidate tumor suppressor gene HIC-1 of a new major alternative TATA-less promoter positively regulated by p53. J Biol Chem 2001;276:3078–89.
7. Chen WY, Wang DH, Yen RC, Luo J, Gu W, Baylin SB. Tumor suppressor HIC1 directly regulates SIRT1 to modulate p53-dependent DNA-damage responses. Cell 2005;123:437–48.
8. Valenta T, Lukas J, Doubravska L, Fafilek B, Korinek V. HIC1 attenuates Wnt signaling by recruitment of TCF-4 and beta-catenin to the nuclear bodies. EMBO J 2006;25:2326–37.
9. Clevers HC, Bevins CL. Paneth cells: maestros of the small intestinal crypts. Annu Rev Physiol 2013;75:289–311.
10. Krausova M, Korinek V. Wnt signaling in adult intestinal stem cells and cancer. Cell Signal 2014;26:570–9.
11. De Sousa EMF, Wang X, Jansen M, Fessler E, Trinh A, de Rooij LP, et al. Poor-prognosis colon cancer is defined by a molecularly distinct subtype and develops from serrated precursor lesions. Nat Med 2013;19:614–8.
12. Briggs KJ, Eberhart CG, Watkins DN. Just say no to ATOH: how HIC1 methylation might predispose medulloblastoma to lineage addiction. Cancer Res 2008;68:8654–6.
13. Van Rechem C, Rood BR, Touka M, Pinte S, Jenal M, Guerardel C, et al. Scavenger chemokine (CXC motif) receptor 7 (CXCR7) is a direct target gene of HIC1 (hypermethylated in cancer 1). J Biol Chem 2009;284: 20927–35.
14. Gerbe F, van Es JH, Makrini L, Brulin B, Mellitzer G, Robine S, et al. Distinct ATOH1 and Neurog3 requirements define tuft cells as a new secretory cell type in the intestinal epithelium. J Cell Biol 2011;192: 767–80.
15. Pospichalova V, Tureckova J, Fafilek B, Vojtechova M, Krausova M, Lukas J, et al. Generation of two modified mouse alleles of the Hic1 tumor suppressor gene. Genesis 2011;49:142–51.
16. Kim S, Karin M. Role of TLR2-dependent inflammation in metastatic progression. Ann N Y Acad Sci 2011;1217:191–206.
17. Tye H, Kennedy CL, Najdovska M, McLeod L, McCormack W, Hughes N, et al. STAT3-driven upregulation of TLR2 promotes gastric tumorigenesis independent of tumor inflammation. Cancer Cell 2012;22:466–78.
18. Campana L, Bosurgi L, Rovere-Querini P. HMGB1: a two-headed signal regulating tumor progression and immunity. Curr Opin Immunol 2008; 20:518–23.
19. Scheeren FA, Kuo AH, van Weele LJ, Cai S, Glykofridis I, Sikandar SS, et al. A cell-intrinsic role for TLR2-MYD88 in intestinal and breast epithelia and oncogenesis. Nat Cell Biol 2014;16:1238–48.

20. el Marjou F, Janssen KP, Chang BH, Li M, Hindie V, Chan L, et al. Tissue-specific and inducible Cre-mediated recombination in the gut epithelium. Genesis 2004;39:186–93.
21. Sato T, Vries RG, Snippert HJ, van de Wetering M, Barker N, Stange DE, et al. Single Lgr5 stem cells build crypt-villus structures *in vitro* without a mesenchymal niche. Nature 2009;459:262–5.
22. Willert K, Brown JD, Danenberg E, Duncan AW, Weissman IL, Reya T, et al. Wnt proteins are lipid-modified and can act as stem cell growth factors. Nature 2003;423:448–52.
23. Melenovsky V, Benes J, Skaroupkova P, Sedmera D, Strnad H, Kolar M, et al. Metabolic characterization of volume overload heart failure due to aorto-caval fistula in rats. Mol Cell Biochem 2011; 354:83–96.
24. Chen EY, Tan CM, Kou Y, Duan Q, Wang Z, Meirelles GV, et al. Enrichr: interactive and collaborative HTML5 gene list enrichment analysis tool. BMC Bioinformatics 2013;14:128.
25. Dubuissez M, Faiderbe P, Pinte S, Dehennaut V, Rood BR, Leprince D. The Reelin receptors ApoER2 and VLDLR are direct target genes of HIC1 (Hypermethylated In Cancer 1). Biochem Biophys Res Commun 2013; 440:424–30.
26. Fafilek B, Krausova M, Vojtechova M, Pospichalova V, Tumova L, Sloncova E, et al. Troy, a tumor necrosis factor receptor family member, interacts with lgr5 to inhibit wnt signaling in intestinal stem cells. Gastroenterology 2013;144:381–91.
27. Waaler J, Machon O, Tumova L, Dinh H, Korinek V, Wilson SR, et al. A novel tankyrase inhibitor decreases canonical Wnt signaling in colon carcinoma cells and reduces tumor growth in conditional APC mutant mice. Cancer Res 2012;72:2822–32.
28. Doubravska L, Krausova M, Gradl D, Vojtechova M, Tumova L, Lukas J, et al. Fatty acid modification of Wnt1 and Wnt3a at serine is prerequisite for lipidation at cysteine and is essential for Wnt signalling. Cell Signal 2011;23:837–48.
29. Lukas J, Mazna P, Valenta T, Doubravska L, Pospichalova V, Vojtechova M, et al. Dazap2 modulates transcription driven by the Wnt effector TCF-4. Nucleic Acids Res 2009;37:3007–20.
30. Kerr MK. Linear models for microarray data analysis: hidden similarities and differences. J Comput Biol 2003;10:891–901.
31. Ventura A, Kirsch DG, McLaughlin ME, Tuveson DA, Grimm J, Lintault L, et al. Restoration of p53 function leads to tumour regression *in vivo*. Nature 2007;445:661–5.
32. Indra AK, Warot X, Brocard J, Bornert JM, Xiao JH, Chambon P, et al. Temporally-controlled site-specific mutagenesis in the basal layer of the epidermis: comparison of the recombinase activity of the tamoxifen-inducible Cre-ER(T) and Cre-ER(T2) recombinases. Nucleic Acids Res 1999;27:4324–7.
33. Dehennaut V, Loison I, Boulay G, Van Rechem C, Leprince D. Identification of p21 (CIP1/WAF1) as a direct target gene of HIC1 (Hypermethylated In Cancer 1). Biochem Biophys Res Commun 2013;430: 49–53.
34. Slattery ML, Herrick JS, Bondurant KL, Wolff RK. Toll-like receptor genes and their association with colon and rectal cancer development and prognosis. Int J Cancer 2012;130:2974–80.
35. Matsuda A, Suzuki Y, Honda G, Muramatsu S, Matsuzaki O, Nagano Y, et al. Large-scale identification and characterization of human genes that activate NF-kappaB and MAPK signaling pathways. Oncogene 2003; 22:3307–18.
36. Aliprantis AO, Yang RB, Mark MR, Suggett S, Devaux B, Radolf JD, et al. Cell activation and apoptosis by bacterial lipoproteins through toll-like receptor-2. Science 1999;285:736–9.
37. Takeuchi O, Kaufmann A, Grote K, Kawai T, Hoshino K, Morr M, et al. Cutting edge: preferentially the R-stereoisomer of the mycoplasmal lipopeptide macrophage-activating lipopeptide-2 activates immune cells through a toll-like receptor 2- and MyD88-dependent signaling pathway. J Immunol 2000;164:554–7.
38. Faure E, Thomas L, Xu H, Medvedev A, Equils O, Arditi M. Bacterial lipopolysaccharide and IFN-gamma induce Toll-like receptor 2 and Toll-like receptor 4 expression in human endothelial cells: role of NF-kappa B activation. J Immunol 2001;166:2018–24.
39. Mohammad HP, Zhang W, Prevas HS, Leadem BR, Zhang M, Herman JG, et al. Loss of a single Hic1 allele accelerates polyp formation in Apc (Delta716) mice. Oncogene 2011;30:2659–69.
40. Grivennikov SI, Karin M. Dangerous liaisons: STAT3 and NF-kappaB collaboration and crosstalk in cancer. Cytokine Growth Factor Rev 2010; 21:11–9.
41. Hausmann M, Kiessling S, Mestermann S, Webb G, Spottl T, Andus T, et al. Toll-like receptors 2 and 4 are up-regulated during intestinal inflammation. Gastroenterology 2002;122:1987–2000.
42. Frolova L, Drastich P, Rossmann P, Klimesova K, Tlaskalova-Hogenova H. Expression of Toll-like receptor 2 (TLR2), TLR4, and CD14 in biopsy samples of patients with inflammatory bowel diseases: upregulated expression of TLR2 in terminal ileum of patients with ulcerative colitis. J Histochem Cytochem 2008;56:267–74.
43. Maeda S, Hikiba Y, Sakamoto K, Nakagawa H, Hirata Y, Hayakawa Y, et al. Colon cancer-derived factors activate NF-kappaB in myeloid cells via TLR2 to link inflammation and tumorigenesis. Mol Med Rep 2011; 4:1083–8.
44. Rakoff-Nahoum S, Medzhitov R. Regulation of spontaneous intestinal tumorigenesis through the adaptor protein MyD88. Science 2007;317: 124–7.
45. el-Deiry WS, Tokino T, Velculescu VE, Levy DB, Parsons R, Trent JM, et al. WAF1, a potential mediator of p53 tumor suppression. Cell 1993;75:817–25.
46. Britschgi C, Rizzi M, Grob TJ, Tschan MP, Hugli B, Reddy VA, et al. Identification of the p53 family-responsive element in the promoter region of the tumor suppressor gene hypermethylated in cancer 1. Oncogene 2006;25:2030–9.
47. Abbas T, Dutta A. p21 in cancer: intricate networks and multiple activities. Nat Rev Cancer 2009;9:400–14.